THE JOURNAL OF BIOLOGICAL CHEMISTRY
Vol. 277, No. 49, Issue of December 6, pp. 47325–47330, 2002

Printed in U.S.A.

X-ray Structure of Two Crystalline Forms of a *Streptomycete* Ribonuclease with Cytotoxic Activity*

Received for publication, August 18, 2002
Published, JBC Papers in Press, September 11, 2002, DOI 10.1074/jbc.M208425200

Jozef Sevcik‡§, Lubica Urbanikova‡, Peter A. Leland¶‖, and Ronald T. Raines¶‡‡**

*From the ‡Institute of Molecular Biology, Slovak Academy of Sciences, Dubravska cesta 21, 84251 Bratislava, Slovak Republic, and the Departments of ¶Biochemistry and **Chemistry, University of Wisconsin-Madison, Madison, Wisconsin 53706*

Ribonuclease (RNase) Sa3 is secreted by the Gram-positive bacterium *Streptomyces aureofaciens*. The enzyme catalyzes the cleavage of RNA on the 3′ side of guanosine residues. Here, x-ray diffraction analysis was used to determine the three-dimensional structure of two distinct crystalline forms of RNase Sa3 to a resolution of 2.0 and 1.7 Å. These two structures are similar to each other as well as to that of a homolog, RNase Sa. All of the key active-site residues of RNase Sa (Asn^{42}, Glu^{44}, Glu^{57}, Arg^{72}, and His^{88}) are located in the putative active site of RNase Sa3. Also herein, RNase Sa3 is shown to be toxic to human erythroleukemia cells in culture. Like onconase, which is an amphibian ribonuclease in Phase III clinical trials as a cancer chemotherapeutic, RNase Sa3 is not inhibited by the cytosolic ribonuclease inhibitor protein. Thus, a prokaryotic ribonuclease can be toxic to mammalian cells.

RNase Sa was the first ribonuclease to be isolated from the growth medium of a Gram-positive microorganism, *Streptomyces aureofaciens* (1). *Streptomycete* ribonucleases belong to the prokaryotic subfamily of microbial ribonucleases of the T1 family, which was identified by Hartley over twenty years ago (2). Amino acid sequence identity between *Streptomycete* ribonucleases and barnase, the best characterized member of the family, is low. Yet, their active sites have a similar structure (3).

After its amino acid sequence was determined (4), RNase Sa became the object of intense structural studies designed to reveal its catalytic mechanism (5–8) and conformational properties (9–12). The level of the enzyme in its natural source is low, and its isolation is tedious. Approaches using recombinant DNA were necessary to obtain adequate quantities of RNase Sa. Consequently, genes encoding two RNase Sa homologs, RNase Sa2 (13) and RNase Sa3 (14), were cloned from *S. aureofaciens* strains R8/26 and CCM 3239, respectively.

Isolation of Sa ribonucleases after the expression of their genes in *Escherichia coli* has not been successful. Apparently, the enzymes are toxic to host cells despite their being directed for secretion. Successful heterologous production has been achieved only by the simultaneous expression of an Sa ribonuclease gene together with a gene encoding barstar, a protein inhibitor from *Bacillus amyloliquefaciens* (15). The yields range from 10 to 50 mg of protein/liter of culture medium (16). Barstar inhibits the enzymatic activity of Sa ribonucleases as it does barnase, its native partner, by sterically blocking the active site (17, 18). Dissociation constants of the complexes of RNase Sa, Sa2, and Sa3 with barstar are 2×10^{-10}, 4×10^{-10}, and 2×10^{-12} M, respectively. For comparison, the dissociation constant for the barnase/barstar complex is 10^{-14} M (15).

The cytosol of mammalian cells contains a ribonuclease inhibitor (RI)[1] protein that binds tightly to mammalian secretory ribonucleases (19, 20). The ability of secretory ribonucleases from human (21), cow (22–24), bull (25–27), and frog (28) to evade RI endows them with toxicity for mammalian cells. These secretory ribonucleases from vertebrates are not homologous to microbial ribonucleases. We suspected that a microbial secretory ribonuclease, such as RNase Sa3, could likewise be toxic to mammalian cells if its structure enables it to evade RI.

Here, we report the atomic structure of two crystalline forms for RNase Sa3. We also report that RNase Sa3 does indeed have the ability to evade RI and is cytotoxic for human erythroleukemia cells. Thus, RNase Sa3 is a prokaryotic ribonuclease with demonstrable cytotoxic activity.

EXPERIMENTAL PROCEDURES

Protein Crystallization—Protein production, purification, and crystallization were performed as described previously (29). The hanging-drop vapor-diffusion method was used to prepare two crystalline forms. Trigonal crystals (crystal I) in the $P3_121$ space group with unit-cell dimensions of $a = b = 64.72$ Å, $c = 69.57$ Å, and $\beta = 120°$ were grown using 0.10 M Hepes buffer, pH 7.6, containing Li_2SO_4 (1.6 M) as the precipitant solution. Hanging drops consisted of 0.05 M Tris-HCl buffer, pH 8.2, containing protein (7.5 mg ml^{-1}), Hepes (0.05 M), and Li_2SO_4 (0.8 M). Tetragonal crystals (crystal II) in the $P4_12_12$ space group with unit-cell dimensions of $a = b = 34.05$ Å and $c = 147.22$ Å were grown using 2-methyl-2,4-pentanediol (10%, v/v) and ammonium sulfate (40 mM) as the precipitant solution. Hanging drops consisted of 20 mM sodium acetate, 2 mM calcium acetate buffer, pH 4.2, containing protein (10 mg ml^{-1}), 2-methyl-2,4-pentanediol (5%, v/v), and ammonium sulfate (20 mM).

Crystallography Data Collection and Processing—X-ray diffraction data collection and processing were performed as described previously (29). Data from crystal I were collected to 2.0 Å at 100 K using synchrotron facilities at EMBL (Hamburg, Germany), and data from crys-

* This work was supported in part by Howard Hughes Medical Institute Grant 75195-547601, Slovak Academy of Sciences Grant 2/1018/21, and National Institutes of Health Grant CA73808. The costs of publication of this article were defrayed in part by the payment of page charges. This article must therefore be hereby marked "*advertisement*" in accordance with 18 U.S.C. Section 1734 solely to indicate this fact.

The atomic coordinates and structure factors (code 1MGW and 1MGR) have been deposited in the Protein Data Bank, Research Collaboratory for Structural Bioinformatics, Rutgers University, New Brunswick, NJ (http://www.rcsb.org/).

§ To whom correspondence may be addressed. Tel.: 42-125-930-7435; Fax: 42-125-930-7416; E-mail: umbisevc@savba.sk.

‖ Supported by Molecular Biosciences Training Grant T32 GM07215 from the National Institutes of Health and a Steenbock/Wharton fellowship from the Department of Biochemistry at the University of Wisconsin-Madison.

‡‡ To whom correspondence may be addressed: Dept. of Biochemistry, University of Wisconsin-Madison, 433 Babcock Dr., Madison, WI 53706-1544. Tel.: 608-262-8588; Fax: 608-262-3453; E-mail: raines@biochem.wisc.edu.

[1] The abbreviations used are: RI, ribonuclease inhibitor; hRI, human ribonuclease inhibitor; r.m.s., root mean square.

TABLE I
Summary of crystallographic refinement and model statistics
ESU, estimated standard uncertainty.

	Structure I	Structure II
Resolution range (Å)	29.6–2.0	20.0–1.7
Temperature (K)	100	293
Unique reflections	11,779	10,355
R_{free} (%)	21.4	22.4
R (%)	15.4	18.6
Protein atoms	782	774
Solvent molecules	145	49
Li^+ ion	1	—
SO_4^{2-} ion	—	1
Average B-factors (Å^2)		
Main chain	28.82	24.75
Side chain	31.31	27.42
Protein atoms	30.05	26.08
Solvent molecules	42.34	35.82
Wilson plot estimate (Å^2)	28.50	22.23
ESU based on R (Å)	0.176	0.188
ESU based on R_{free} (Å)	0.125	0.112
r.m.s. deviation from ideal geometry (target values in parentheses)		
Bond distances (Å)	0.021 (0.021)	0.020 (0.021)
Bond angles (°)	1.831 (1.931)	1.783 (1.932)
Chiral centers (Å^3)	0.105 (0.200)	0.119 (0.200)
Planar groups (Å)	0.008 (0.020)	0.008 (0.020)
Main-chain bond B values (Å^2)	1.642 (1.500)	2.067 (1.500)
Main-chain angle B values (Å^2)	2.560 (2.000)	3.129 (2.000)
Side-chain bond B values (Å^2)	3.836 (3.000)	3.880 (3.000)
Side-chain angle B values (Å^2)	5.842 (4.500)	5.728 (4.500)
Residues in Ramachandran plot regions (excluding Pro, Gly, and terminal residues)		
Most favored (%)	93.9	93.6
Additional allowed (%)	6.1	6.4

tal II were collected likewise to 1.7 Å at room temperature. Data were processed with the HKL package (30). Data sets from both crystalline forms were 100% complete with R_{merge} values of 6.0 and 3.6% for crystals I and II, respectively.

Protein Structure Determination and Refinement—The structures from crystals I (structure I) and II (structure II) were determined by molecular replacement using the program AMoRe (31) and the structure of RNase Sa as a search model (Protein Data Bank entry 1RGG). The initial model yielded for structure I an R-factor of 46% and a correlation coefficient of 51.7% for data at 10–3 Å. The initial model yielded for structure II an R-factor of 47% and a correlation coefficient of 45.0% for data at 10–3 Å. Molecular replacement showed clearly that there was one protein molecule in the asymmetric unit in both structures (29).

Individual atomic refinement was performed against 95% of the data by using the maximum likelihood program REFMAC5 (version 4.1) from the CCP4 package (32) against 95% of the data. The remaining 5% of the data randomly excluded from the full data set by the program Uniqueify from the CCP4 package was used for cross-validation by means of the R_{free} factor (33). The last refinement cycle was carried out against all of the data. The Sparse Matrix method was used for minimization. After each refinement cycle, the automated refinement procedure ARP/wARP (34) was applied for modeling and updating the solvent structure. The models were inspected against $3F_o - 2F_c$ and $F_o - F_c$ maps and adjusted manually between the cycles of refinement with the program O (35).

Both structures were refined with isotropic and, in later stages, anisotropic temperature factors including contributions to the structure factors from the hydrogen atoms, which were generated in standard geometries. The inclusion of hydrogen atoms lowered the values of R and R_{free} by >1 unit. Isotropic and anisotropic temperature factors, bond lengths, and bond angles were restrained according to the standard criteria employed by REFMAC5.

Assay of Ribonuclease Inhibitor Binding—Human ribonuclease inhibitor (hRI) and RNase A were from Sigma. hRI was stored in 20 mM Hepes-KOH buffer, pH 7.6, containing glycerol (50%, v/v), KCl (50 mM), and dithiothreitol (8 mM). The effect of hRI on ribonucleolytic activity was measured as described previously (36) with minor modifications. RNase Sa3 was incubated with hRI for 5 min at room temperature. The enzymatic reaction was initiated at 37 °C by the addition of substrate. The reaction mixture (1.0 ml) was 0.10 M sodium phosphate buffer, pH 7.5, containing a ribonuclease (RNase Sa3, RNase Sa, or RNase A), hRI, yeast RNA (3 mg), EDTA (1.0 mM), and dithiothreitol (5 mM). After 15 min, the enzymatic reaction was terminated by cooling the reaction mixture on ice for 2 min and then adding a solution (0.25 ml) of uranylacetate (0.75% w/v) in aqueous perchloric acid (25% v/v). The quenched reaction mixture was subjected to centrifugation, and the supernatant was diluted by 25-fold with distilled water before recording its absorbance at 260 nm. The concentration of ribonuclease in the reaction mixture was adjusted to give an increase in absorbance at 260 nm of 0.2–0.3 cm^{-1} in the absence of hRI.

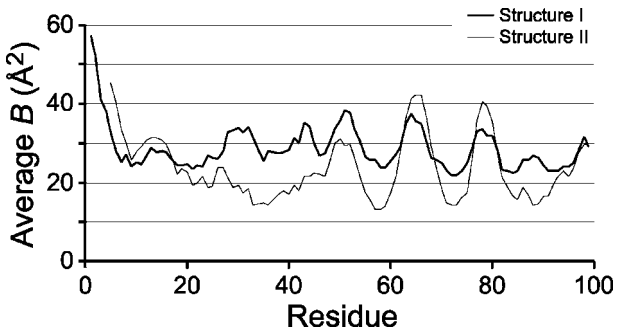

FIG. 1. **Average temperature factors of RNase Sa3 structures I and II as a function of residue number.**

Assay of Cytotoxicity—Onconase (22) and RNase Sa3 (16) were prepared as described previously. K-562 cells, which are from a continuous human chronic myelogenous leukemia line, were from the American Type Culture Collection (Manassas, VA). The effect of ribonucleases on the proliferation of K-562 cells was determined by measuring the incorporation of [*methyl*-^{3}H]thymidine into cellular DNA as described previously (22, 37) with the exception that the stock solution of ribonucleases was in 10 mM sodium phosphate buffer, pH 8.0, containing NaCl (0.10 M). Data represent the average of quadruplicate samples within an individual assay. The IC_{50} value of each cytotoxic ribonuclease was calculated by using the equation: $S = 100 \times IC_{50}/(IC_{50} + [\text{ribonuclease}])$ where S is the percent of total DNA synthesis after the incubation period (24).

RESULTS AND DISCUSSION

Quality of Final Protein Structure Models—The starting R-factors in the refinement were 46.5% (48.3%) for structure I (structure II). Refinement converged with R- and R_{free} factors

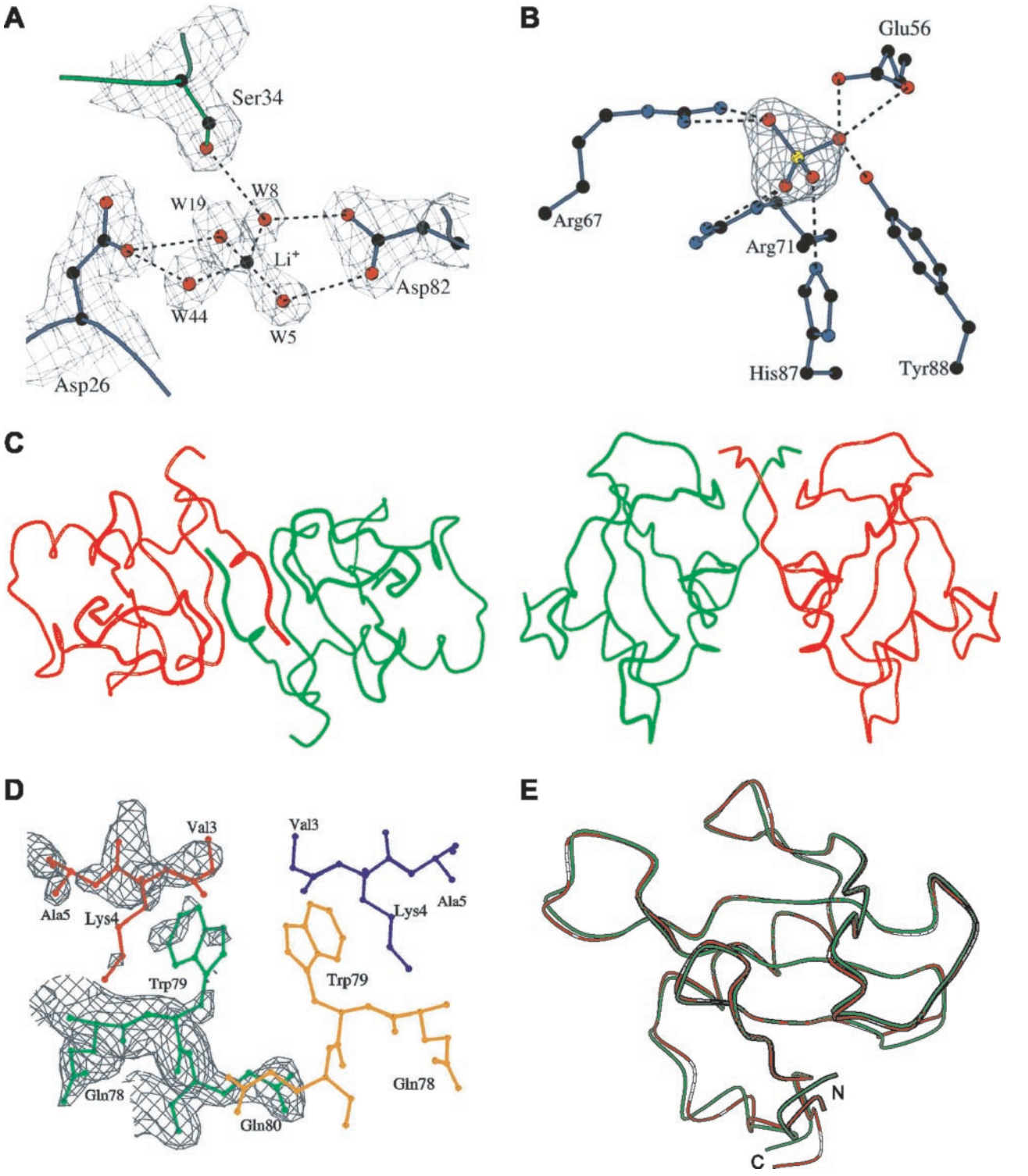

FIG. 2. **Three-dimensional structure of RNase Sa3.** *A*, electron density of lithium ion of RNase Sa3 structure I in the middle of a tetrahedron formed by four water molecules. Putative hydrogen bonds are denoted by *broken lines*. Ser^{34} is from a molecule related by symmetry. *B*, electron density of sulfate anion of RNase Sa3 structure II at the 1σ level and putative hydrogen bonds with neighboring residues. For clarity, electron density of the residues is omitted. *C*, two views of the interaction of two adjacent RNase Sa3 molecules in structure I. *D*, contact region of four RNase Sa3 molecules in structure II. For clarity, electron density at the 0.3σ level for residues from only two molecules is shown. *E*, superposition of RNase Sa (*red*) (8) and RNase Sa3 structure I (*green*) based on 37 core C_α atoms. *Panels A*, *B*, and *D* were produced with the program Bobscript (57). *Panels C* and *E* were produced with Molscript (58).

of 15.4% (18.6%) and 21.4% (22.4%), respectively. Both models have good geometry with r.m.s. deviations from ideal bond lengths and angles of 0.021 Å (0.020 Å) and 1.831° (1.783°). 93.9% (93.6%) of the ψ and ϕ dihedral angles were in the most favored region of the Ramachandran plot (38) as calculated with the program Procheck (39). None of the residues was in a disallowed region. For both structures, the dispersion precision indicator (59, 60) based on the values of *R*- and R_{free} factors yields estimated standard uncertainty (ESU) <0.19 and <0.13 Å, respectively. The atomic coordinates of structure I and structure II of RNase Sa3 have been deposited in the Protein Data Bank with accession codes 1MGW and 1MGR, respectively.

```
Sa3   ASVKAVGRVCYSALPSQAHDTLDLIDEGGPFPY  33
Sa    -DVS--GTVCLSALPPEATDTLNLIASDGPFPY  30
                                *     *

                 _ _                _
Sa3   SQDGVVFQNREGLLPAHSTGYYHEYTVITPGSP  66
Sa    SQDGVVFQNRESVLPTQSYGYYHEYTVITPGAR  63
         *   * ***   **         *

               _                   _
Sa3   TRGARRIITGQQWQEDYYTADHYASFRRVDFAC  99
Sa    TRGTRRIITGEATQEDYYTGDHYATFSLIDQTC  96
        *    *              * ***   *
```

FIG. 3. **Amino acid sequences of RNase Sa3 and RNase Sa.** Residues conserved in all microbial ribonucleases are denoted by "—," and those conserved in the prokaryotic subfamily are denoted by an *asterisk*.

The crystallographic refinement and model statistics are listed in Table I. The average temperature factors for main-chain atoms for both structures as a function of residue number are shown in Fig. 1. Surprisingly, the *B*-factors are lower for structure II (room temperature data) than for structure I (100 K data), which can be explained by the lower water content in crystal forms II (34%) and I (68%). The average *B*-factors agree well with estimates from the Wilson plot (61). The pattern of variation is similar for both structures, but the amplitude of variation is larger for structure II. The quality of the electron density in the interior of both structures is approximately equal despite the different resolutions and conditions for data collection.

Description of Protein Structures—Recombinant RNase Sa3 consists of 99 amino acid residues. The main secondary structure elements are an α-helix (residues 18–28) and a three-stranded antiparallel β-sheet (residues 55–61, 72–78, and 82–87). The protein belongs to the Alpha Beta Roll group of the CATH classification of protein domain structures (40). The final model for structure I contains 782 protein atoms and 145 water molecules. The final model for structure II contains 774 protein atoms and 49 water molecules. The peptide bond preceding Pro^{30} is in the *cis*-conformation. The enzyme contains two cysteine residues in positions 10 and 99, which form a disulfide bond.

In structure I, all residues were built, and there are no residues with alternative conformations. A difference electron density was seen after all refinement cycles in the middle of four water molecules arranged in the corners of a tetrahedron. A lithium cation was modeled at the site of difference electron density and refined as shown in Fig. 2*A*. The distances to respective water molecules are 1.8–2.0 Å. The *B*-factors of water molecules and the Li^+ ion are 30–36 and 16 $Å^2$, respectively.

In structure II, residues Ala^1, Ser^2, and the side chain of Val^3 (which together form an N-terminal tail) are missing, because there was no electron density clear enough to model these residues. The electron density for Lys^4 and Trp^{79} side chains was poor, resulting in temperature factors of up to 60 $Å^2$. Alternative conformations were built for the O_γ atom of Ser^{12}. A sulfate anion SO_4^{2-} was modeled at the putative phosphoryl group binding site as shown in Fig. 2*B* in analogy to one found in RNase Sa (8). The average S–O bond length was 1.45 Å.

The room temperature and low temperature structures are almost identical. An overlap of the two structures based on the minimization of distances between 94 C_α atoms (excluding the five N-terminal C_α atoms) yields an r.m.s. displacement of 0.50 Å with a maximum displacement of 1.75 Å at the Trp^{79} side chain.

Crystal Packing and Lattice Interactions—In structure I, each molecule makes intermolecular contacts with three neighbors. The crystal consists of a lattice of molecules that form continuous parallel chains between those that are large channels of the solvent corresponding to 68% crystal volume. Between each pair of chains, every third molecule forms close intermolecular contacts with its partner from the neighboring chain. As shown in Fig. 2*C*, the N-terminal loops of two neighboring molecules are intertwined and trapped between the two molecules, forming a number of contacts that prevent disorder.

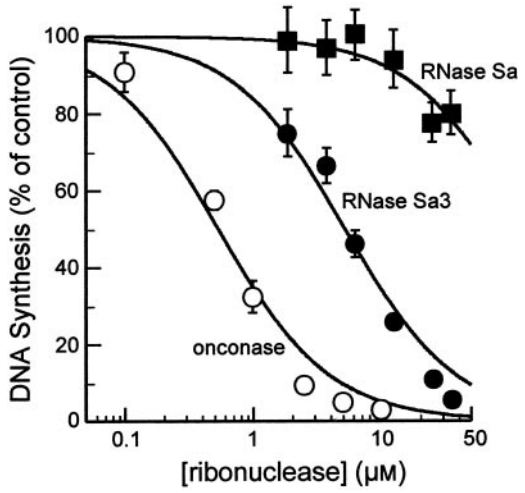

FIG. 4. **Effect of onconase, RNase Sa3, and RNase Sa on the proliferation of K-562 cells.** Cell proliferation was measured by incorporation of [*methyl*-^{3}H]thymidine into cellular DNA after a 48-h incubation at 37 °C with a ribonuclease. Each value is the mean (±S.E.) of at least three independent experiments with triplicate samples and is expressed as a percentage of the control, which lacked a ribonuclease. IC_{50} values are 0.43 ± 0.04 μM (onconase), 5 ± 1 μM (RNase Sa3), and >35 μM (RNase Sa).

In structure II, each molecule makes intermolecular contacts with 12 neighboring molecules. The molecules are packed closely, which results in a solvent content of only 34%. It is interesting to note that four neighboring molecules in the crystal face each other with disordered regions. As shown in Fig. 2*D*, this interface contains N-terminal residues of two molecules and Trp^{79} residues of two other molecules. The disorder of these regions is surprising as the space in the interface does not seem to be large enough to allow for substantial atomic motion.

Comparison with Other Ribonuclease Structures—Sa ribonucleases catalyze the cleavage of the P–$O^{5'}$ bonds of single-stranded RNA on the 3′ side of guanosine nucleotides (62). The most thoroughly studied *Streptomycete* ribonuclease is RNase Sa, the structure of which was determined at various resolutions, including atomic. As shown in Fig. 3, a comparison of the amino acid sequences of RNase Sa and RNase Sa3 reveals that there are 67 identical residues (69% identity), 17 of which are conserved in all enzymes belonging to the prokaryotic subfamily of microbial ribonucleases. There are five key residues: Asn^{42}, Glu^{44}, Glu^{57}, Arg^{72}, and His^{88} (Sa3 numbering) that are conserved strictly in all microbial ribonucleases of the T1 family. By analogy, Glu^{57} and His^{88} participate in general acid base catalysis. Glu^{44} and Arg^{72} participate in nucleobase and phosphoryl group binding, respectively. The side chain of Asn^{42} plays an important role in stabilizing the main-chain loop that forms the binding site for the nucleobase of a substrate. Replacing an equivalent asparagine residue in RNase Sa with aspartate, alanine, or serine decreases the conformational stability of the enzyme by 1.5–2.3 kcal/mol (9) and decreases the catalytic activity by 85%.[2] The N39S variant of RNase Sa also shows unexpected changes in structure (Protein Data Bank code 1BOX).

An overlap of RNase Sa3 structure I with the structure of RNase Sa based on minimization of distances between those corresponding C_α atoms that form the core of the molecules (37

[2] L. Urbanikova, unpublished data.

atoms) yields an r.m.s. deviation of 0.35 Å and a maximum deviation of 0.84 Å, which is the distance between the C_α atoms of Gly^{28} (Sa3) and Asp^{25} (Sa). This superposition reveals a high degree of similarity as depicted in Fig. 2*E*. Differences in the main-chain fold are seen only at the N and C termini and reached 5 and 2 Å, respectively. The N-terminal residues of RNase Sa are well determined as they are laid on the surface of the molecule. The situation is different in RNase Sa3 in which the N-terminal residues form a tail that does not contact the remainder of the molecule but instead points to the solution.

Ribonuclease Inhibitor Binding—Previously, the ribonuclease inhibitor protein was demonstrated to have no effect on the ribonucleolytic activity of microbial ribonucleases T1 and U1 (41). In the conditions used herein, hRI was able to fully inactivate RNase A but had no effect on the activity of RNase Sa and Sa3, even at a 10-fold greater concentration. Thus, streptomycete ribonucleases Sa and Sa3 bind tightly to barstar (15) but evade hRI.

Cytotoxicity—RNase Sa3 exhibits dose-dependent toxicity to K-562 cells as shown in Fig. 4. The IC_{50} value for RNase Sa3 is (5 ± 1) μM, which is only 10-fold greater than that of onconase. In contrast to RNase Sa3, RNase Sa does not exhibit significant cytotoxic activity.

Ribonucleases can be cytotoxic by virtue of their ribonucleolytic activity. The cytotoxic activity of some vertebrate ribonucleases has led to their development as cancer chemotherapeutics (42–44). For example, onconase, which is the homolog of RNase A in the Northern leopard frog (*Rana pipiens*), is now in Phase III clinical trials for the treatment of malignant mesothelioma, a form of lung cancer (45). A few fungal ribonucleases are also known to have antitumor activity (46). Specifically, the *Aspergillus* ribonucleases α-sarcin (47), mitogillin (48), restrictocin (49), and Asp-fl (50) kill cells by cleaving a specific phosphodiester bond in 28 S rRNA, thereby disrupting the ribosome and impairing protein biosynthesis (51).

To our knowledge, RNase Sa3 is only the second prokaryotic ribonuclease to have demonstrable cytotoxic activity (63). The mechanism by which RNase Sa3 manifests its cytotoxicity is unclear but probably relies on its ribonucleolytic activity as does the cytotoxicity of other ribonucleases (52). The three-dimensional structure of RNase Sa3, which is highly similar to that of its non-toxic homolog RNase Sa (Fig. 2*E*), provides no obvious clues. Likewise, the conformational stability of the two ribonucleases, which can correlate with cytotoxicity (53), is similar (11). However, the endogenous ability of RNase Sa3 to evade RI is reminiscent of that of onconase (28) and bovine seminal ribonuclease (54), two mammalian ribonucleases with cytotoxic activity. This ability is also probably critical for the cytotoxicity of RNase Sa3. Furthermore, RNase Sa3 is more cationic than is RNase Sa (pI = 5.4 and 3.5, respectively) (16), and more cationic ribonucleases are more cytotoxic (55). Additional studies are necessary to reveal the basis as well as the mechanism of RNase Sa3 cytotoxicity. These studies are compelled by the need to develop new cytotoxins for use in cell biology and medicine (43, 56).

Acknowledgments—We are grateful to C. N. Pace for contributive discussions. We thank EMBL in Hamburg for providing facilities on beamlines X31 and BW7A. J. Sevcik and L. Urbanikova thank the European Community for support through the Access to Research Infrastructure Action of the Improving Human Potential Program to the EMBL Hamburg Outstation (contract number HPRI-CT-1999-00017).

REFERENCES

1. Bacova, M., Zelinkova, E., and Zelinka, J. (1971) *Biochim. Biophys. Acta* **235,** 335–338
2. Hartley, R. W. (1980) *J. Mol. Evol.* **15,** 355–358
3. Sevcik, J., Sanishvili, R. G., Pavlovsky, A. G., and Polyakov, K. M. (1990) *Trends Biochem. Sci.* **15,** 158–162
4. Shlyapnikov, S. V., Both, V., Kulikov, V. A., Dementiev, A. A., Sevcik, J., and Zelinka, J. (1986) *FEBS Lett.* **209,** 335–339
5. Sevcik, J., Dodson, E. J., and Dodson, G. G. (1991) *Acta Crystallogr. B* **47,** 240–253
6. Sevcik, J., Hill, C. P., Dauter, Z., and Wilson, K. S. (1993) *Acta Crystallogr. D* **49,** 257–271
7. Sevcik, J., Zegers, I., Wyns, L., Dauter, Z., and Wilson, K. S. (1993) *Eur. J. Biochem.* **216,** 301–305
8. Sevcik, J., Dauter, Z., Lamzin, V. S., and Wilson, K. S. (1996) *Acta Crystallogr. D* **52,** 327–344
9. Hebert, E. J., Giletto, A., Sevcík, J., Urbániková, L., Wilson, K. S., Dauter, Z., and Pace, C. N. (1998) *Biochemistry* **37,** 16192–16200
10. Pace, C. N., Alston, R. W., and Shaw, K. L. (2000) *Protein Sci.* **9,** 1395–1398
11. Pace, C. N., Horn, G., Hebert, E. J., Bechert, J., Shaw, K., Urbanikova, L., Scholtz, J. M., and Sevcik, J. (2001) *J. Mol. Biol.* **312,** 393–404
12. Shaw, K. L., Grimsley, G. R., Yakovlev, G. I., Makarov, A. A., and Pace, C. N. (2001) *Protein Sci.* **10,** 1206–1215
13. Nazarov, V. (1991) Cloning the genes coding for extracellular ribonuclease and its inhibitor from *Streptomyces aureofaciens*, Ph.D. thesis, Institute of Molecular Biology, Bratislava, Slovak Republic
14. Homerova, D., Hollanderova, Z., Kormanec, J., and Sevcik, J. (1992) *Gene* (*Amst.*) **119,** 147–148
15. Hartley, R. W., Both, V., Hebert, E. J., Homerova, D., Jucovic, M., Nazarov, V., Rybajlak, I., and Sevcik, J. (1996) *Protein Pept. Lett.* **4,** 225–231
16. Hebert, E. J., Grimsley, G. R., Hartley, R. W., Horn, G., Schell, D., Garcia, S., Both, V., Sevcik, J., and Pace, C. N. (1997) *Protein Expression Purif.* **11,** 162–168
17. Sevcik, J., Urbanikova, L., Dauter, Z., and Wilson, K. S. (1998) *Acta Crystallogr. D* **54,** 954–963
18. Urbanikova, L., and Sevcik, J. (1998) *Acta Crystallogr. D* **54,** 403–404
19. Hofsteenge, J. (1997) in *Ribonucleases: Structures and Functions* (D'Alessio, G., and Riordan, J. F., eds), pp. 621–658, Academic Press, New York
20. Shapiro, R. (2001) *Methods Enzymol.* **341,** 611–628
21. Leland, P. A., Staniszewski, K. E., Kim, B.-M., and Raines, R. T. (2001) *J. Biol. Chem.* **276,** 43095–43102
22. Leland, P. A., Schultz, L. W., Kim, B.-M., and Raines, R. T. (1998) *Proc. Natl. Acad. Sci. U. S. A.* **98,** 10407–10412
23. Bretscher, L. E., Abel, R. L., and Raines, R. T. (2000) *J. Biol. Chem.* **275,** 9893–9896
24. Haigis, M. C., Kurten, E. L., Abel, R. L., and Raines, R. T. (2002) *J. Biol. Chem.* **277,** 11576–11581
25. Cafaro, B., De Lorenzo, C., Piccoli, R., Bracale, A., Mastronicola, M. R., Di Donato, A., and D'Alessio, G. (1995) *FEBS Lett.* **359,** 31–34
26. Kim, J.-S., Soucek, J., Matousek, J., and Raines, R. T. (1995) *J. Biol. Chem.* **270,** 10525–10530
27. Matousek, J., Kim, J.-S., Soucek, J., Rihà, J., Ribò, M., Leland, P. A., and Raines, R. T. (1997) *Comp. Biochem. Physiol.* **118B,** 881–888
28. Wu, Y., Mikulski, S. M., Ardelt, W., Rybak, S. M., and Youle, R. J. (1993) *J. Biol. Chem.* **268,** 10686–10693
29. Hlinkova, V., Urbanikova, L., Krajcikova, D., and Sevcik, J. (2001) *Acta Crystallogr. D* **57,** 737–739
30. Otwinowski, Z., and Minor, W. (1997) *Methods Enzymol.* **276,** 307–326
31. Navaza, J., and Saludjian, P. (1997) *Methods Enzymol.* **276,** 581–619
32. Collaborative Computational Project Number 4 (1994) *Acta Crystallogr. D* **50,** 760–763
33. Brünger, A. T. (1993) *Acta Crystallogr. D* **49,** 24–36
34. Perrakis, A., Morris, R. M., and Lamzin, V. S. (1999) *Nat. Struct. Biol.* **6,** 458–463
35. Jones, T. A., Zou, J. Y., Cowan, S. W., and Kjeldgaard, M. (1991) *Acta Crystallogr. A* **47,** 110–119
36. Egami, F., Takahashi, K., and Uchida, T. (1964) *Prog. Nucleic Acid Res. Mol. Biol.* **3,** 59–101
37. Leland, P. A., Staniszewski, K. E., Kim, B.-M., and Raines, R. T. (2000) *FEBS Lett.* **477,** 203–207
38. Ramakhrisnan, C., and Ramachandran, G. M. (1965) *Biophys. J.* **5,** 909–933
39. Laskowski, R. A., MacArthur, M. W., Moss, D. S., and Thornton, J. M. (1993) *J. Appl. Crystallogr.* **26,** 283–291
40. Orengo, C. A., Michie, A. D., Jones, S., Jones, B. T., Swindells, M. B., and Thornton, J. M. (1997) *Structure* **5,** 1093–1108
41. Cho, S., and Joshi, J. G. (1989) *Anal. Biochem.* **176,** 175–179
42. Youle, R. J., and D'Alessio, G. (1997) in *Ribonucleases: Structures and Functions* (D'Alessio, G., and Riordan, J. F., eds), pp. 491–514, Academic Press, New York
43. Leland, P. A., and Raines, R. T. (2001) *Chem. Biol.* **8,** 405–413
44. Matousek, J. (2001) *Comp. Biochem. Physiol. C Toxicol. Pharmacol.* **129,** 175–191
45. Mikulski, S. M., Costanzi, J. J., Vogelzang, N. J., McCachren, S., Taub, R. N., Chun, H., Mittelman, A., Panella, T., Puccio, C., Fine, R., and Shogen, K. (2002) *J. Clin. Oncol.* **20,** 274–281
46. Wool, I. G. (1997) in *Ribonucleases: Structures and Functionsv* (D'Alessio, G., and Riordan, J. F., eds), pp. 131–162, Academic Press, New York
47. Pérez-Cañadillas, J. M., Santoro, J., Campos-Olivas, R., Lacadena, J., Martínez del Pozo, A., Gavilanes, J. G., Rico, M., and Bruix, M. (2000) *J. Mol. Biol.* **299,** 1061–1073
48. Kao, R., and Davies, J. (1999) *J. Biol. Chem.* **274,** 12576–12582
49. Yang, X., and Moffat, K. (1996) *Structure* **4,** 837–852
50. Madan, T., Arora, N., and Sarma, P. U. (1997) *Mol. Cell. Biochem.* **175,** 21–27
51. Schindler, D. G., and Davies, J. E. (1977) *Nucleic Acids Res.* **4,** 1097–1100
52. Kim, J.-S., Soucek, J., Matousek, J., and Raines, R. T. (1995) *Biochem. J.* **308,** 547–550
53. Klink, T. A., and Raines, R. T. (2000) *J. Biol. Chem.* **275,** 17463–17467
54. Murthy, B. S., and Sirdeshmukh, R. (1992) *Biochem. J.* **281,** 343–348
55. Futami, J., Maeda, T., Kitazoe, M., Nukui, E., Tada, H., Seno, M., Kosaka, M.,

and Yamada, H. (2001) *Biochemistry* **26,** 7518–7524
56. Rappuoli, R., and Montecucco, C. (1997) *Guidebook to Protein Toxins and Their Use in Cell Biology*, Oxford University Press, New York
57. Esnouf, R. M. (1999) *Acta Crystallogr. D* **55,** 938–940
58. Kraulis, P. J. (1991) *J. Appl. Crystallogr.* **24,** 946–950
59. Cruickshank, D. W. J. (1996) in *Proceedings of the CCP4 Study Weekend, Macromolecular Refinement* (Dodson, E., Moore, M., Ralph, A., and Bailey, S., eds) pp. 11–22, SERC Daresbury Laboratory, Warrington, United Kingdom
60. Murshudov, G. N., and Dodson, E. J. (1997) *CCP4 Newslett. Protein Crystallogr.* **33,** 31–39
61. Wilson, A. J. C. (1942) *Nature* **150,** 151–152
62. Zelinkova, E., Bacova, M., and Zelinka, J. (1971) *Biochim. Biophys. Acta* **235,** 343–352
63. Ilinskaya, O., Decker, K., Koshinski, A., Dreyer, F., and Repp, H. (2001) *Toxicology* **156,** 101–107